

A methodology to model and simulate customized realistic anthropomorphic robotic hands

Tian, Li; Magnenat-Thalmann, Nadia; Thalmann, Daniel; Zheng, Jianmin

2018

Tian, L., Magnenat-Thalmann, N., Thalmann, D., & Zheng, J. (2018). A methodology to model and simulate customized realistic anthropomorphic robotic hands. Proceedings of Computer Graphics International 2018, 153-162. doi:10.1145/3208159.3208182

<https://hdl.handle.net/10356/138936>

<https://doi.org/10.1145/3208159.3208182>

© 2018 Association for Computing Machinery. All rights reserved. This paper was published in CGI 2018: Proceedings of Computer Graphics International 2018 and is made available with permission of Association for Computing Machinery.

Downloaded on 20 Mar 2024 20:11:09 SGT

A Methodology to Model and Simulate Customized Realistic Anthropomorphic Robotic Hands

Li Tian
Nanyang Technological University
Singapore
tianli@ntu.edu.sg

Nadia Magnenat-Thalmann
Nanyang Technological University
Singapore
nadiathalmann@ntu.edu.sg

Daniel Thalmann
EPFL
Switzerland
daniel.thalmann@epfl.ch

Jianmin Zheng
Nanyang Technological University
Singapore
asjmzheng@ntu.edu.sg

ABSTRACT

When building robotic hands, researchers are always face with two main issues of how to make robotic hands look human-like and how to make robotic hands function like real hands. Most existing solutions solve these issues by manually modelling the robotic hand [10-18]. However, the design processes are long, and it is difficult to duplicate the geometry shape of a human hand. To solve these two issues, this paper presents a simple and effective method that combines 3D printing and digitization techniques to create a 3D printable cable-driven robotic hand from scanning a physical hand. The method involves segmenting the 3D scanned hand model, adding joints, and converting it into a 3D printable model. Comparing to other robotic solutions, our solution retains more than 90% geometry information of a human hand¹, which is attained from 3D scanning. Our modelling progress takes around 15 minutes that include 10 minutes of 3D scanning and five minutes for changing the scanned model to an articulated model by running our algorithm. Compared to other articulated modelling solutions [19, 20], our solution is compatible with an actuation system which provides our robotic hand with the ability to mimic different gestures. We have also developed a way of representing hand skeletons based on the hand anthropometric. As a proof of concept, we demonstrate our robotic hand's performance in the grasping experiments.

CCS CONCEPTS

• **Computer systems organization** → **Robotics**; Embedded systems

KEYWORDS

Customised robotic hand, hand anthropometric, 3D printing, 3D scanning, cable-driven actuation

ACM Reference format:

L. Tian, N. Magnenat-Thalmann, D. Thalmann and J. Zheng. 2018. SIG Proceedings Paper in word Format. In *Computer Graphics International 2018, Bintan Island, Indonesia*, 10 pages. <https://doi.org/10.1145/3208159.3208182>

1 INTRODUCTION

This paper considers the problem of creating customized human robotic realistic hands, which should not only function like a human hand, but also have similar shape, size and appearance as the target. The techniques for creating such hands are very useful in making hands for disable people and robotics (especially social robots) as well. However, the problem is challenging since it by nature involves 3D modeling, manufacturing, and mechanics. Moreover, the complexity of hand structures and functions makes the problem even tougher.

Human body has 244 Degree of Freedoms (DOFs) which are controlled by 630 muscles [1]. DOFs are most concentrated in human hands which contribute a total of 54 DOFs [2]. Besides high dexterity, human hands are also quite strong and good at grasping. A male adult's grip strength is generally up to 50 kg [3]. Human hands are complex and have inspired many different designs of robotic hands [4]. However, when evaluating the hand's DOFs, range of motion of each joint, accuracy, speed, grasping trajectory, grasping force, weight, and appearance, so far no robotic hand could fully match the human hand [5]. The main challenge comes from three aspects: 1) The human hand is covered with skin which is elastic with a freeform shape [2]. 2) The human hand has a complex mechanism that is combined with bones, muscles, tendons, ligaments and so on. The modellings of robotic hands usually do not include soft tissues such as muscles and ligaments. It is thus complicated to simulate all mechanical properties to a robotic hand model [2, 5]. 3) With reference to the actuators, the current artificial muscle solutions are still not as

¹ Calculate by hand's surface area

Permission to make digital or hard copies of all or part of this work for personal or classroom use is granted without fee provided that copies are not made or distributed for profit or commercial advantage and that copies bear this notice and the full citation on the first page. Copyrights for components of this work owned by others than ACM must be honored. Abstracting with credit is permitted. To copy otherwise, or republish, to post on servers or to redistribute to lists, requires prior specific permission and/or a fee. Request permissions from [Permissions@acm.org](https://doi.org/10.1145/3208159.3208182).
CGI 2018, June 11–14, 2018, Bintan Island, Indonesia
© 2018 Association for Computing Machinery. ACM ISBN 978-1-4503-6401-0/18/06...\$15.00 <https://doi.org/10.1145/3208159.3208182>

efficient as the human muscles which require more space to provide the same amount of force [6].

Inspired by the advance of 3D scanning and 3D printing technologies, this paper proposes a new solution to creating customized human robotic realistic hand [7]. Our solution consists of digitization, 3D modeling, and mechanical control design. Specifically, we first use a 3D scanner to scan a physical hand, which produces a 3D mesh model with high accuracy as the base model of our robotic hand. Then we design an algorithm to convert the scanned 3D mesh model into an interlocked articulated 3D model that can be printed out by a 3D printer. Finally, for the actuation, we use six high-torque (3.7 kg/cm) but tiny (20x18x30mm) and light (12.7 grams) servo motors with specially designed servo bed as the control solution of our robotic hand to simulate the motion of the human hand. Compared to exiting work, our approach is simpler and more effective.



Fig. 1 (Top) 3D-printed scanned hand and real hand (Bottom) our robotic hand and its 3D model

The rest of the paper is organised as follows: Section 2 gives an overview of existing related work about robotic hands. Section 3 presents our design process and fabrication in detail. Section 4 reports our experiments of evaluating the performance of the design in terms of grasping objects, followed by our conclusion and future work in Section 5.

2 Related Work

This section briefly reviews related work in three categories: Prosthetic Robotic Hand, Research Purpose Robotic Hand, and Automation of Articulated Joint.

2.1 Prosthetic Robotic Hand

The commercial prosthetic hands are mainly designed for disabled people to help them manipulate objects from daily life. Grasping is the most important gesture which refers to a static posture with

an object held securely with one hand [8]. In 1989, Cutkosky categorized human grasps into 15 different postures [9]. However, most prosthetic hands can only simulate a few of them due to the constraints of cost, weight and robust design for long-term use.

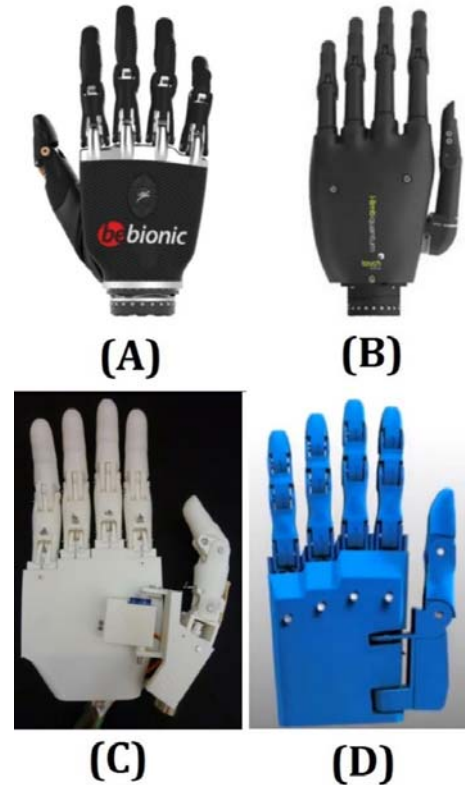


Fig. 2 Prosthetic Robotic Hand (A) Bebionic hand[10], (B) i-Limb hand[5], (C) Tact hand[11] and (D) Dextrus hand[12].

Due to their purpose, prosthetic hands usually are made of metal parts linked by screws and actuated by motors[5]. They look like human hands with five separated fingers but are generally heavier than a real hand. We compare their weight with our robotic hand in Table 1. Designs of Bebionic hand [10], Limb hand [5] and Tact hand [11] use 11 joints and 6 DOFs. For this design, the thumb has three joints and two DOFs while other fingers have two joints with one DOF. The Dextrus hand uses 15 joints and six DOFs [12]. All Dextrus hand's fingers have three joints, giving it a more human-like grasp. Tact hand and Dextrus hand are 3D printable, and the cost is lower than the other two [11] [12].

Table 1 Mass comparison of the robotic hands

Robotic Hand Name	Developer	Mass (g)
Our robotic hand (2018)	(* hide)	175
InMoov Hand (2015) [13]	Gael Langevin	400
Tact (2015) [11]	University of Illinois	350
Dextrus (2013) [12]	Open Hand Project	428

Bebionic (2014) [10]	RSL steeper	550
i-Limb (2010) [5]	Touch Bionic	460-465
Xu et al's hand (2016) [14]	Xu et. al.	942

For all these hands, the parts need to be designed separately. It is time-consuming and the manually modelled appearance is not very similar to the human hand. Our proposed method aims to solve these two issues.

2.2 Robotic Hand for Research Purpose

Since the first dexterous hand, the Stanford/JPL hand, was created in 1983 [15], many researchers has used a real hand as the golden sample which is created by nature [16]. The research oriented robotic hands have the design intention different from the prosthetic robotic hand. They have no limitation on the weight, size of the control system or the way they are linked to the human arm. So they can focus on simulating a certain aspect of human hands as identically as possible.

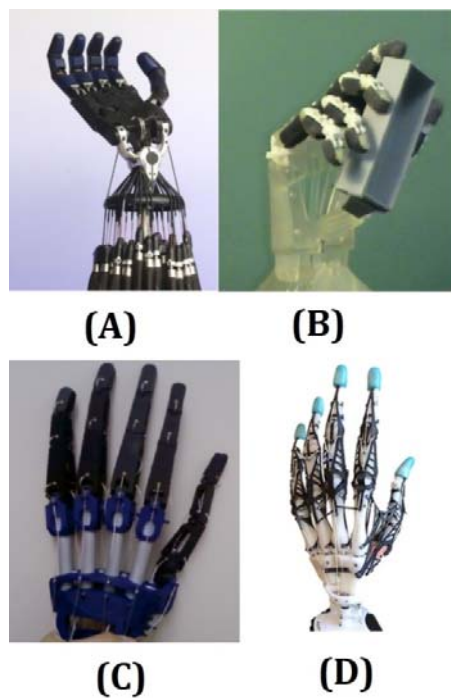


Fig.3 Research Purpose robotic hand (A) Shadow hand [17] (B) UB hand IV [18] (C) Xu et al's anthropomorphic robotic hand [19], and (D) Xu et al's highly biomimetic robotic [14]

The Shadow hand has a large actuation system which includes up to 40 actuators. The shadow hand has 20 DOFs which are close to the DOFs of a real hand. The UB hand IV has human-like fingers which are driven by 24 twisted-string actuators. Z. Xu has designed two robotic hands, of which are based on the bones structure of a hand [14, 19]. He designed a low-cost modular, 20-DOF anthropomorphic robotic hand in 2013 [19] (see Figure 3C) and a highly biomimetic robotic hand which simulates finger ligaments with soft tissues in 2016 [14] (see Figure 3D).

All these robotic hands use ten or more actuators to drive the fingers. A large and heavy control system will limit the application of the robotic hand. Different from these hands, we reduce the DOFs and create a simplified mechanical hand model without losing much functionality.

2.3 Automation of Articulated Joint

In addition to manual modelling, there are solutions to creating the joints for the 3D model automatically. In [20] a method is proposed to convert 3D models into printable, functional, non-assembly models with internal friction. The approach takes an appropriately rigged 3D model, automatically fits novel 3D-printable and posable joints, and provides an interface for specifying rotational constraints. It can create an interlocked hand without the need for manual assembly of joint components (Fig. 4A).

Another approach [21] takes a skinned mesh as input, and then estimates a single-material model that approximates the 3D kinematics of the corresponding virtual articulated character in a piecewise linear manner (see Fig. 4B).

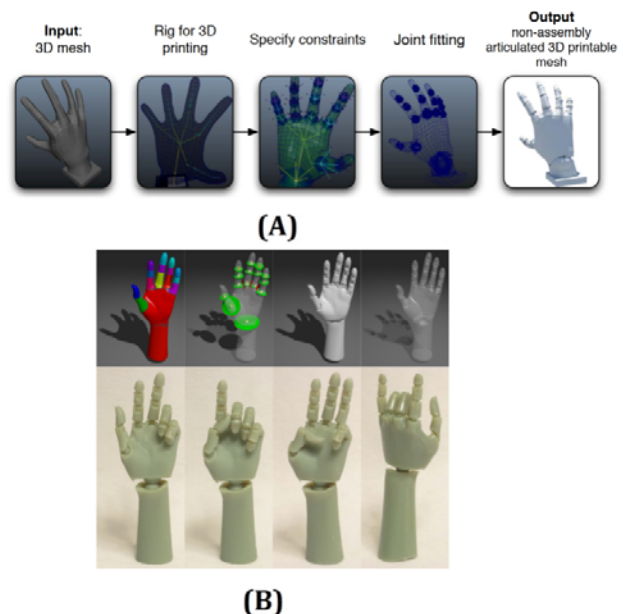


Fig.4 (A) 3D-Printing of Non-Assembly, Articulated Models[20] (B) Fabricating Articulated Characters from Skinned Meshes [21]

The two methods above provide automatic ways to create robotic hands. However, the final models are both rigid and difficult to add actuators. Therefore, they are articulated hand models but not robotic hands. Compared to these methods, our method not only provides a way to create the joints of the hand but also takes care of the motion control, which makes our robotic hand possible by a cable-driven system. The way to locate joints in this paper is also differ with these two previous works.

3 Our method

This section explains our approach in detail. We first study the biomechanical features of a human hand such as the bones and joints that provide the guidance for creating a robotic hand model in order to simulate important features of the hand. We also apply the constraints of the human hand to simplify its range of motion without significantly reducing its functionalities. Next, we design our new 3D hand model based on our understanding of hand motions. Finally, we implement our design to a 3D hand model through a Python script code.

3.1 Human hand mechanism and limitation

A normal human hand has a total of 27 bones [2]. Five bones are in the palm, 14 bones support five fingers, and the remaining eight bones are located in the wrist. The hand also has 15 movable joints, and each finger has three. The three joints of the thumb are distal-interphalangeal (DIP) joint, metacarpophalangeal (MCP) joint, and trapeziometacarpal (TM) joint (also known as carpometacarpal (CMC) joint). The joints of the other four fingers consist of three joints, DIP joint, proximal interphalangeal (PIP) joint, and MCP joint (Fig 5A, 5B). All 15 joints have a DOF in the flexion and extension direction. All five MCP joints and the only TM joint have one additional DOF in adduction and abduction direction. In total, the human hand has 27 DOFs that includes six more DOFs are contributed by the wrist (Fig 5C).

Due to the natural mechanism of the human hand, all 21 DOFs have different range of motion. Past research has shown that the five MCP's adduction and abduction motions are limited within the range of 0 – 30 degrees [22]. According to hand grasp taxonomy, they are relatively unimportant in the grasping action [23, 24]. We neglect these five DOFs when designing our robotic hand. Except for the thumb, other four fingers' DIP and PIP are controlled by the same tendon named “flexor digitorum profundus tendon” [2]. Most gestures are required to move each finger's three joints together [24]. As the thumb plays the most important role in grasping [24], we have simplified it to two DOFs and other four fingers to one DOF for our robotic hand. In figure 5D, five vertical red lines represent five DOFs of fingers flexion and extension motion. Each DOF controls the three finger joints together. The horizontal red line (at the TM joint) represents one additional DOF which controls the abduction and adduction move of the thumb. We will show our control system in details in Section 3.4 Actuation System.

Based on the placement of hand bones, we can segment the hand into several linked sections [25]. Prior research shows that these segments are rather proportionate with small deviations [25, 26]. Therefore, we can either estimate the dimension of each segment by the proportions or measure them simply with a ruler. Section 3.3 will show how we set landmarks and how we use them for modelling our robotic hand.

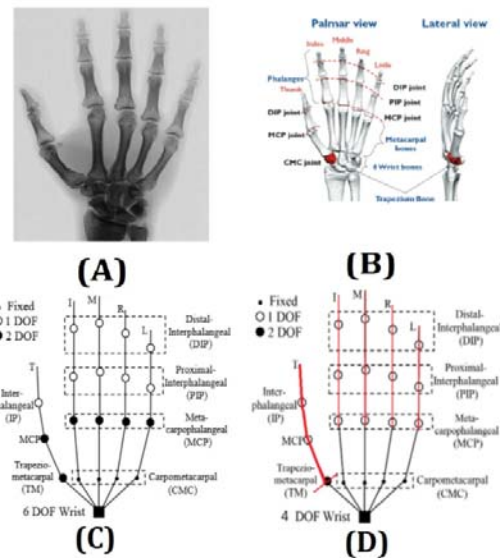


Fig. 5 Bones in human hand (A, B) [2], hand's 27 DOFs (C) [27] and mechanical model of our robotic hand (6 DOFs) (D) [27]

3.2 3D scanning and hollowing

Compared to manual 3D modelling, 3D scanning is a quick and accurate way of getting a 3D hand model. The scanned target can be a real human hand or even an artificial silicon hand skin. We scanned a real human hand using a handheld 3D scanner “Artec Space Spider”. The 3D scanned model can be represented in different formats. Here, we use triangle mesh in stereolithography (STL) format.

The first step we need to take is to make the hand hollow. We use software “MeshMixer” to separate the hand model from the wrist and set the thickness to 1.5mm. The thickness will greatly affect the strength and the weight of the final robotic hand. We used 2mm and 1.5mm, and we conclude that 1.5mm is sufficient for print with Acrylonitrile Butadiene Styrene (ABS). We printed a 3D scanned hand model, which is shown in Figure 1.

3.3 Hand Modelling

Similar to other mechanisms, a hand needs the joint structure for the centripetal movement. The joints in human hands have a complex biological structure, whereas the bones are linked by ligaments. Between them, there are articular cartilage, synovial cavity and synovial membrane. All of these are hidden beneath the skin and are difficult to mimic. Our method will provide a general solution to transform from a 3D hand model to an actuated model.

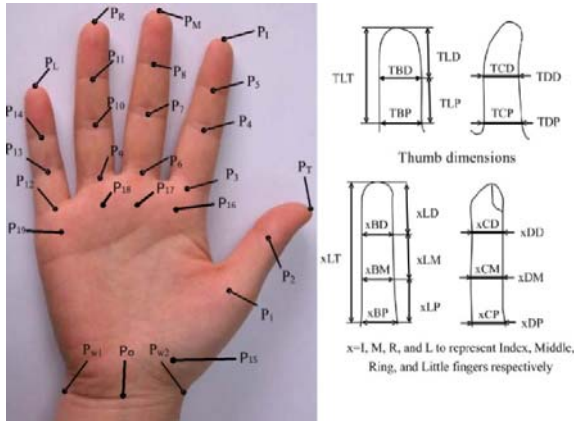


Fig. 6 (left) Landmarks of the hand and (right) dimensions of fingers (amend from [26])

We identified 21 landmarks for in human hand (Fig. 5) based on previous research [26]. After which, we added six more landmarks. Five of these are P_{15} to P_{19} which represent the positions of the thumb's TM joint and MCP joints of the other four fingers. The details of these notations can be found in the appendix. The landmark " P_o " is the original point of the hand, which is located at the bottom end of the capitate bone. It is almost at the middle point of P_{w1} and P_{w2} .



Fig. 7 Movable joints of human hand (in green dot)

To make the 3D hand articulable, we need to divide the hand into segments and apply joints to link these segments. As the hand has 15 movable joints, we need the precise positions to implement the joints. Here we provide a simple way to calculate them. Here a simple way on how to calculate them has been provided. From Figure 7, based on a hand X-ray photos, we marked the 15 movable joints of the human hand in the green dot, which are similar to corresponding hand landmarks. For each finger, we draw lines from the tips to the point " P_o " with four straight segments passing through three movable joints. We get a total of 20 segments in four layers. Starting from the original point; we call them first to fourth layers.

We can get the length of the hand from the line (P_M , P_o) either from a real hand or a 3D hand model. We also can calculate the

length of each finger bone, metacarpals and the length of Capitate. The ratio and the calculation results of a 180 millimeter hand are shown in table 3 at the end. Here we choose 180 millimeter (mm) as a previous study (<http://www.theaveragebody.com>) found that hand sizes for males range from 159 mm to 206 mm, and we rounded up the average to 180 mm.

$$xLy = HLT \times Rxy \quad (1)$$

$$HTL = HTL \times (RMM + RMP + RMI + RMD) + CVL \quad (2)$$

We name the joints at the end of the first layer "Root joint". We set the segment (P_{17} , P_o) as the central line of the hand and make it vertical to "xz plane" (Fig. 7). Human's Metacarpals are not exactly straight. However, the offset is not significant [2]. So we assume all five root joints and P_o are in the same plane with zero z coordinate. As the wrist's breadth and wrist circumference decide the palm size and the position of the root joints, we then assume the four angles made from (P_{17} , P_o) and the other four segments from the palm can be calculated from the HTL. (One of angle "AMI" is marked in yellow in figure 7) So we can use bellow formula to calculate the 3D coordinate of root joints' landmark.

For P_{16} - P_{19} :

$$\begin{aligned} P_aX &= xLM \times \sin \frac{AMx \times \pi}{180} \\ P_aY &= xLM \times \cos \frac{AMx \times \pi}{180} \\ P_aZ &= 0 \end{aligned} \quad (3)$$

$a = 16, 17, 18$ or 19 . X, Y, Z are the 3D coordinates from P_o

For thumb's P_{15} , we find that the segment (P_{15} , P_o) is slightly larger than CVL, and we set offset to correct the value. Currently, we have set it to 2 millimetres under the condition of $HLT = 180$ millimeters. The ratio is yet to be proven.

$$\begin{aligned} P_{15}X &= (CVL + \frac{HLT \times 2}{180}) \times \sin \frac{ATO \times \pi}{180} \\ P_{15}Y &= (CVL + \frac{HLT \times 2}{180}) \times \cos \frac{ATO \times \pi}{180} \\ P_{15}Z &= 0 \end{aligned} \quad (4)$$

We can place our finger in an ideal position when 3D scanning. The two requirements are: 1. All 15 movable joints' landmarks are on the same plane with zero z coordinate. 2. All landmarks in each finger lay on a straight line. We can calculate the rest of the landmark positions using the same way as root joint, and all of this calculation is based on one input, HTL. Here, the way to calculate the position of the remaining landmarks based on the five root joints was also provided. For example, to calculate the P_3 , P_4 , P_5 and P_1 , from the human hand limitation, we get

$$\begin{aligned} 0^\circ \leq AFP_3, AFP_5 \leq 90^\circ \\ 0^\circ \leq AFP_4 \leq 110^\circ \\ -15^\circ \leq AAP_3 \leq 15^\circ \\ AAP_4, AAP_5 = 0^\circ \end{aligned} \quad (5)$$

Hence, we need the value of AFP_3 , AFP_4 , AFP_5 and AAP_3 for further calculation based on the equation of a sphere.

$$P_4X = P_{16}X + ILP \times \sin \frac{AFP_{16} \times \pi}{180} \times \sin \frac{AAP_{16} \times \pi}{180}$$

$$\begin{aligned} P_4 Y &= P_{16} Y + ILP \times \sin \frac{AFP_{16} \times \pi}{180} \times \cos \frac{AAP_{16} \times \pi}{180} \\ P_4 Z &= P_{16} Z + ILP \times \cos \frac{AFP_{16} \times \pi}{180} \end{aligned} \quad (6)$$

We can use the same method to get the coordinate of the other landmarks.

To validate our method, we implement our algorithm in Maya with Python script. We placed the hollowed hand model with the “Po” point overlapping the original point with coordinates (0,0,0) in Maya. We also set the segment (P₁₇, P_o) vertical to “xz plane”. Then, we run our Python script to edit the 3D hand model. In our code, we input HTL as well as necessary angles if the hand model is not in the ideal case. Next, we calculate the position of the movable joints and the dimension of the hand. After that, we cut the finger into 15 pieces based on the position of points P₁ – P₁₅. We use these 15 landmarks as reference points to place 15 blocks to each knuckle’s positions. In order to make a gap between the neighbours’ knuckles, the blocks are slightly shorter than knuckles, so different knuckles will be 3D printed in different parts. Then, we create 15 joints structure for the 15 hand’s movable joints. The thumb’s TM joint uses ball joint mechanism to meet the two DOFs requirement, while other 14 joints use the hinged design for one DOF. Each hinge joint is made out of five standard objects. The upper connector is a cylinder which is linked to the upper knuckle (red lines as shown in Figure 8). It is also linked to two other cylinders called middle connector and lower connector. The two pipes are linked with the lower knuckle. They are precisely placed, surrounding the lower connector with a 1-millimeter gap. This design allows the upper knuckle to rotate using the lower connector as a rotating shaft. The sizes of these parts depend on the dimensions that were calculated above.

Most existing robotic hands mimic the MCP joint motion with the axis of rotation at the endpoint of four fingers (except the thumb). For example, with reference to Figure 6, the MCP joints of the four fingers are placed at the landmark P₃, P₆, P₉ and P₁₂. However, according to the human hand anatomy (Fig. 5), the MCP joints are inside the palm with the position of landmark P₁₆, P₁₇, P₁₈ and P₁₉. We use these points as references to add the rotating shafts.

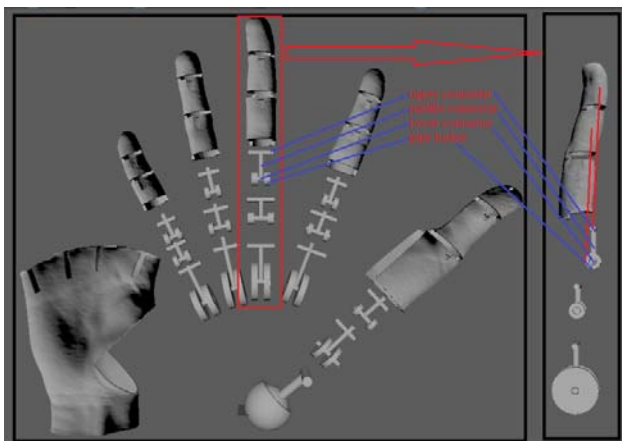


Fig. 8 (left) Front view of inside structure of our robotic hand (right) Side view of middle finger

For the thumb’s TM joint, it has two DOFs, and both of them are important for grasping. The ball joint is a common design in our daily life and is already applied on robotic hands [28]. Here, we show our method of using script code to create a ball joint in Maya in Figure 9.

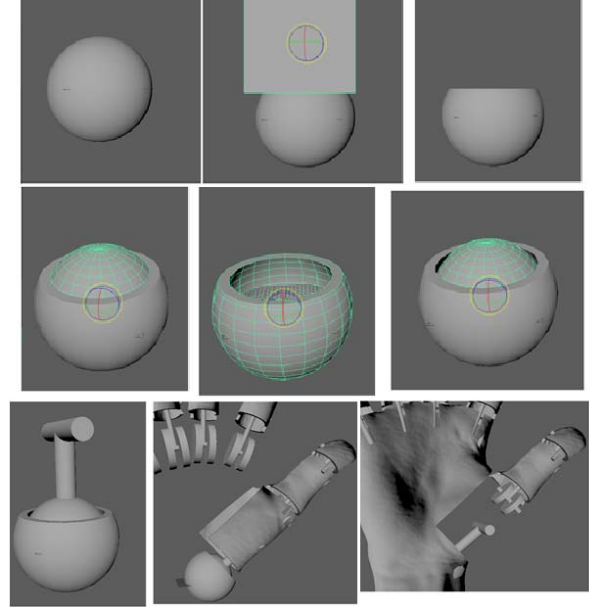


Fig. 9 Steps to creating the ball joint for TM joint

We also use Maya to simulate the collision caused by the finger motion. As our hinge joint target range of motion is 0 to 90 degrees, we simulate the motion of fingers with the same range of motion to identify overlapping of the neighbouring parts. Then, we remove the colliding parts which could obstruct the motion. Finally, we add holes to all five fingertips for the control cables, and we get the interlocked robotic hand model ready for 3D printing. We 3D printed it out and the experiment result is shown in Section 4.

3.4 Actuation System

Electric and pneumatic motors are two widely used actuators for robotic hands while linkages, camshafts, gears and cables are common tools for transmitting the force from the actuator to fingers [5]. Although there are several artificial muscles such as [29], we still choose electric servo motor and cable-driven method for our actuation solution because of their high efficiency and low cost [30].

We use 0.5mm diameter Nylon as our robotic hand tendon. One side of the cable is tied outside the fingertips. The knot is covered with reusable putty-like adhesive so that it will increase the friction between the fingertips and the target objects. The cable goes through the inside of the fingers and the palm. The other side of the cable is tied to the horn of the motor. When the motor’s horn starts to turn, the finger will move from the DIP joint which has the smallest resistance. Then PIP and MCP joints will be actuated in sequence. Figure 9 shows how the motors actuate the middle finger and the thumb. The range of motion is controlled by our algorithm which results in a human-like hand motion.

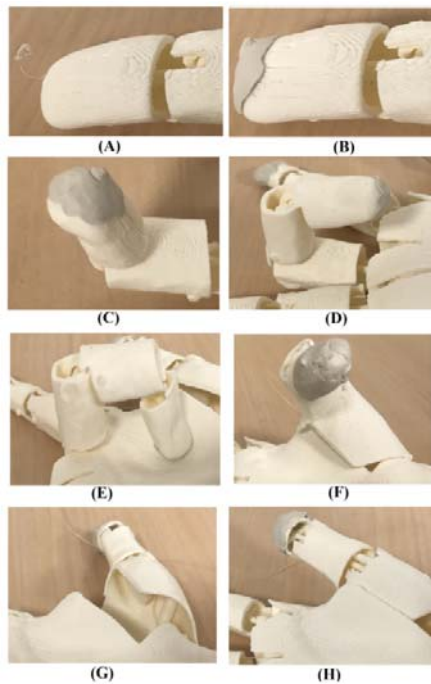


Fig. 10 Cable-driven finger

4 Experiments

We conduct experiments to evaluate our robotic hand. We first test the weight and range of motion of our robotic hand. Then, we do the grasping test individually and with a humanoid robot.

4.1 Weight Control

Lightweight is one of our design priorities. Weight is important especially when the robotic hand has been integrated with the humanoid robot. According to the previous test result, our realistic humanoid robot's forearm motion would be obviously affected when the mass of the linked robotic hand is heavier than 500 grams. We 3D print our robotic hand with "uPrint SE Plus" 3D Printer. The hand is printed with ABS material of high density and weighs only 72 grams. We weigh our robotic hand and compare it with others in Table 1. According to the table, our robotic hand is the lightest because we use hollow design with the thin shell (1.5mm). Our actuator server motor, HITEC HS-5070MH, is also tiny and light (12.7g). The total weight of the robotic hand is 175 grams including servos, servo bed and 3D hand model, and the artificial skin weight is 127g.

4.2 Range of motion of Fingers

We test our robotic hand's range of motion for each finger with a comparison with other robotic hands and a real human hand. The results are given in Table 2. While the artificial skin reduces the range of motion of each joint, it greatly improves the appearance and increases the friction of the grasp.

Table 2 Hand joint moving angle

Robotic hand name	MCP	PIP	DIP	TM flexion	TM circumduction
Our robotic hand (With artificial skin)	0-90 (0-70)	0-90 (0-70)	0-90 (0-70)	0-90 (0-70)	0-60 (0-30)
Nadine hand [31]	0-90	0-110	0-90	0-90	0-90
Tact hand[11]	0-90	23-90	20	0-90	0-105
Dextrus hand[12]	0-90	0-90	0-90	0-90	0-120
i-Limb hand[5]	0-90	0-90	20	0-60	0-95
Bebionic hand[10]	0-90	0-90	20	-	0-68
Human hand[32]	90	100	90	70	70

4.3 Grasp Test

For all grasping tests, we place the target objects at a fixed position in front of our robotic hand, and we drive the actuators to control each finger to approach the target objects. A few gestures are generated after multiple trials.



Fig. 11 Grasping test

4.4 Grasp Test with Artificial Skin

The silicon artificial skins can improve the appearance of robotic hands. With our method, we can quickly create a robotic hand that fit the artificial skin. We can either 3D scan the artificial skin to get the basic hand 3D model or 3D scan the real hand (Then use the output 3D model to make the artificial skin). In both case we can make our 3D printed our robotic hand works fine with the artificial skin. As they use same base model.

We test our robotic hand with silicon artificial skin as well as demonstrated that our robotic hand works well with artificial skin in Figure 12. The customised artificial hand skin uses silicon of 0-degree hardness in 1-2mm thickness.

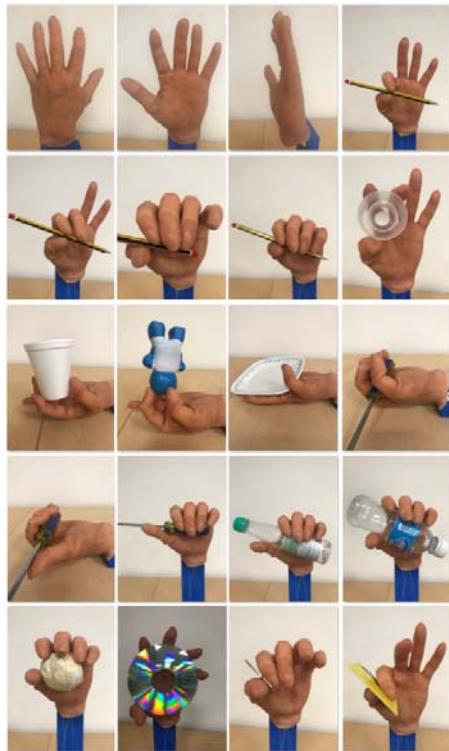


Fig. 12 Grasping test with artificial skin

4.5 Grasp Test with Humanoid Robot

We have tested our robotic hand on an open-sourced humanoid robot [13] and a realistic humanoid robot. The results showed that the robot could grasp the objects as per plotted motions. Figure 13 provides four screenshots of the robot grasp test.

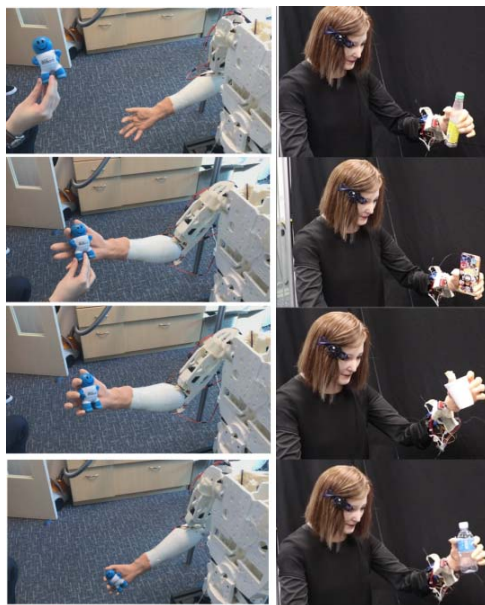


Fig. 13 Grasping test with humanoid robots

Since the first appearance of Virtual Humans in the early 1980s, many types of research related to grasping plan have been conducted in a virtual environment[33]. We have designed a virtual robot based on “Anthropometric Body Modeling”[34]. The virtual robot is a 3D model which has the same scale as the real robot or an adult woman. We added animations to each movable joint to simulate motion. The animation control parameters are manually set to match the motor control parameters, so the motion of the real robot will be replicated by the animation of the virtual robot under the same control parameters. As a result, we can adequately test any grasping actions in the virtual robot before applying it to the real robot. The way of the grasping is based on the “heuristic grasping decision”[35] and the motions of the Nadine robot are pre-set at this stage.



Fig. 14 Four intermediaries' actions of virtual and real robot [27]

5. Conclusions and Future Work

We have described a new method to create a personalized robotic hand. We start with studying how human hand functions, and try to replicate the important features of the 3D hand model using our algorithm. Our algorithm transforms a 3D scanned hand model to an articulated hand model which has similar range of motion as a human hand. Our robotic hand has 15 joints with only a single inter-locked model, so this part of the hand is free of assembly. We set the thickness of the robotic hand printing empirically. In the case of 1.5mm thickness, the created hand weighs only 72 grams. Our robotic hand has six DOFs which are powered by six small-size actuators. The wrist joint can be customized for different robots. The experiments show that our robotic hand is able to express most of the important grasping configurations. Compared to other robotic hands and actuated modelling methods, we have provided a comprehensive procedure on how to automatically create a personalized robotic hand.

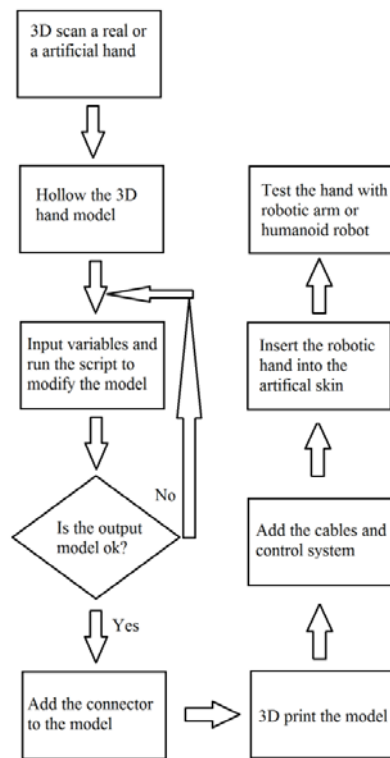


Fig. 15 Flow chart of our Methodology

In the future, we plan to improve our work in several ways:

- 1). Increasing the grasping force and the range of motion of the fingers.
- 2). Integrating visual recognition to its control system to achieve autonomous grasping of objects based on visual information.
- 3). Improving the grasping manner to make it more natural and human-like.

Table 3 Ratio of dimensions of hand and length (HTL=180mm)

No.	Name	Ratio	Result(mm)
1	TLT	0.318	57.23
2	TLP	0.152	27.352
3	TLD	0.166	29.877
4	ILT	0.38	68.486
5	ILD	0.137	24.722
6	ILP	0.13	23.46
7	ILM	0.113	20.304
8	MLT	0.417	75.009
9	MLD	0.14	25.248
10	MLP	0.146	26.195
11	MLM	0.131	23.565
12	RLT	0.388	69.854
13	RLD	0.138	24.828
14	RLP	0.129	23.25
15	RLM	0.121	21.777
16	LLT	0.311	55.967

17	LLD	0.124	22.303
18	LLP	0.102	18.41
19	LLM	0.085	15.254
20	HLT	1	180
21	TBD	0.112	20.199
22	TBP	0.16	28.72
23	TDD	0.096	17.253
24	TDP	0.123	22.092
25	IBD	0.089	16.096
26	IBM	0.105	18.936
27	IBP	0.114	20.514
28	IDD	0.076	13.676
29	IDM	0.092	16.517
30	IDP	0.103	18.515
31	MBD	0.089	16.096
32	MBM	0.105	18.831
33	MBP	0.108	19.357
34	MDD	0.076	13.676
35	MDM	0.095	17.148
36	RBD	0.082	14.728
37	RBM	0.096	17.358
38	RBP	0.103	18.515
39	RDD	0.071	12.729
40	RDM	0.088	15.885
41	LBD	0.076	13.676
42	LBM	0.088	15.78
43	LBP	0.1	17.989
44	LDD	0.069	12.414
45	LDM	0.081	14.623
46	LDP	0.088	15.78
47	MDP	0.117	21.146
48	RDP	0.115	20.725
49	WB	0.323	58.177
50	TCD	0.355	63.857
51	TCP	0.48	86.476
52	ICD	0.287	51.654
53	ICM	0.331	59.544
54	ICP	0.376	67.75
55	MCD	0.289	51.97
56	MCM	0.335	60.386
57	MCP	0.363	65.33
58	RCD	0.265	47.656
59	RCM	0.31	55.757
60	RCP	0.341	61.333
61	LCD	0.249	44.816
62	LCM	0.281	50.602
63	LCP	0.321	57.756
64	WC	0.924	166.324

Acknowledgements

This research is supported by the BeingTogether Centre, a collaboration between Nanyang Technological University (NTU) Singapore and University of North Carolina (UNC) at Chapel Hill. The BeingTogether Centre is supported by the National Research Foundation, Prime Minister's Office, Singapore under its International Research Centres in Singapore Funding Initiative.

REFERENCES

- [1] Zatsiorsky, V. and B. Prilutsky, Biomechanics of skeletal muscles. 2012: Human Kinetics.
- [2] Agur, A.M. and A.F. Dalley, Grant's atlas of anatomy. 2009: Lippincott Williams & Wilkins.
- [3] Mathiowetz, V., et al., Grip and pinch strength: normative data for adults. *Arch Phys Med Rehabil*, 1985. 66(2): p. 69-74.
- [4] Mattar, E., A survey of bio-inspired robotics hands implementation: New directions in dexterous manipulation. *Robotics and Autonomous Systems*, 2013. 61(5): p. 517-544.
- [5] Belter, J.T., et al., Mechanical design and performance specifications of anthropomorphic prosthetic hands: A review. *Journal of Rehabilitation Research and Development*, 2013. 50(5): p. 599-617.
- [6] Ariano, P., et al., Polymeric materials as artificial muscles: an overview. *Journal of applied biomaterials & functional materials*, 2015. 13(1).
- [7] Shah, P.B. and Y. Luximon. Review on 3D Scanners for Head and Face Modeling. in *International Conference on Digital Human Modeling and Applications in Health, Safety, Ergonomics and Risk Management*. 2017. Springer.
- [8] Feix, T., et al. A comprehensive grasp taxonomy. in *Robotics, science and systems: workshop on understanding the human hand for advancing robotic manipulation*. 2009.
- [9] Cutkosky, M.R., On Grasp Choice, Grasp Models, and the Design of Hands for Manufacturing Tasks. *Ieee Transactions on Robotics and Automation*, 1989. 5(3): p. 269-279.
- [10] Medynski, C. and B. Rattray. Bionic prosthetic design. 2011. *Myoelectric Symposium*.
- [11] Slade, P., et al., Tact: Design and Performance of an Open-Source, Affordable, Myoelectric Prosthetic Hand. 2015 *Ieee International Conference on Robotics and Automation (Icra)*, 2015: p. 6451-6456.
- [12] Phillips, B., et al. A review of current upper-limb prostheses for resource constrained settings. in *Global Humanitarian Technology Conference (GHTC)*, 2015 IEEE. 2015. IEEE.
- [13] Langevin, G., InMoov-Open Source 3D printed life-size robot. pp. URL: <http://inmoov.fr>, License: <http://creativecommons.org/licenses/by-nc/3.0/legalcode>, 2014.
- [14] Xu, Z. and E. Todorov, Design of a Highly Biomimetic Anthropomorphic Robotic Hand towards Artificial Limb Regeneration. 2016 *Ieee International Conference on Robotics and Automation (Icra)*, 2016: p. 3485-3492.
- [15] Salisbury, J.K. and B. Roth, Kinematic and force analysis of articulated mechanical hands. *ASME J. Mech., Transm., Autom. Des.*, 1983. 105(1): p. 35-41.
- [16] Kalganova, T., et al., A novel design process of low cost 3D printed ambidextrous finger designed for an ambidextrous robotic hand. 2015.
- [17] Rothling, F., et al. Platform portable anthropomorphic grasping with the bielefeld 20-dof shadow and 9-dof tum hand. in *Intelligent Robots and Systems*, 2007. IROS 2007. IEEE/RSJ International Conference on. 2007. IEEE.
- [18] Melchiorri, C., et al., Development of the ub hand iv: Overview of design solutions and enabling technologies. *IEEE Robotics & Automation Magazine*, 2013. 20(3): p. 72-81.
- [19] Xu, Z., V. Kumar, and E. Todorov. A low-cost and modular, 20-DOF anthropomorphic robotic hand: design, actuation and modeling. in *Humanoid Robots (Humanoids)*, 2013 13th IEEE-RAS International Conference on. 2013. IEEE.
- [20] Cali, J., et al., 3D-Printing of Non-Assembly, Articulated Models. *Acm Transactions on Graphics*, 2012. 31(6).
- [21] Bäcker, M., et al., Fabricating articulated characters from skinned meshes. *ACM Trans. Graph.*, 2012. 31(4): p. 47:1-47:9.
- [22] Lin, J., Y. Wu, and T.S. Huang, Modeling the constraints of human hand motion. *Workshop on Human Motion, Proceedings*, 2000: p. 121-126.
- [23] Feix, T., et al. A comprehensive grasp taxonomy. in *Robotics, science and systems: workshop on understanding the human hand for advancing robotic manipulation*. 2009.
- [24] Feix, T., et al., The grasp taxonomy of human grasp types. *IEEE Transactions on Human-Machine Systems*, 2016. 46(1): p. 66-77.
- [25] Alexander, B. and K. Viktor, Proportions of hand segments. *Int. J. Morphol.*, 2010. 28(3): p. 755-758.
- [26] Li, Z., et al., Validation of a three-dimensional hand scanning and dimension extraction method with dimension data. *Ergonomics*, 2008. 51(11): p. 1672-1692.
- [27] Magnenat Thalmann, N., L. Tian, and F. Yao, Nadine: A Social Robot that Can Localize Objects and Grasp Them in a Human Way, in *Frontiers in Electronic Technologies*. 2017, Springer. p. 1-23.
- [28] Konnaris, C., et al., EthoHand: A Dexterous Robotic Hand with Ball-Joint Thumb Enables Complex In-hand Object Manipulation. 2016 6th Ieee International Conference on Biomedical Robotics and Biomechatronics (Biorob), 2016: p. 1154-1159.
- [29] Dicker, M.P., et al., Light-triggered soft artificial muscles: Molecular-level amplification of actuation control signals. *Scientific reports*, 2017. 7(1): p. 9197.
- [30] Pillay, P. and R. Krishnan, Application characteristics of permanent magnet synchronous and brushless DC motors for servo drives. *IEEE Transactions on industry applications*, 1991. 27(5): p. 986-996.
- [31] Tian, L., et al., The making of a 3D-printed, cable-driven, single-model, lightweight humanoid robotic hand. *Frontiers in Robotics and AI*, 2017. 4: p. 65.
- [32] Lowe, W., *Orthopedic Assessment in Massage Therapy*. 2006: Daviau Scott.
- [33] Magnenat-Thalmann, N. and D. Thalmann, *The Direction of Synthetic Actors in the film Rendez-vous à Montréal*. *IEEE Computer Graphics and applications*, 1987. 7(12): p. 9-19.
- [34] Magnenat-Thalmann, N. and D. Thalmann, *Handbook of virtual humans*. 2005: John Wiley & Sons.
- [35] Huang, Z., et al., A multi-sensor approach for grasping and 3D interaction, in *Computer graphics*. 1995, Elsevier. p. 235-253.